白芍抗抑郁组分在大鼠体内代谢及抑郁对其代谢处置的差异

何昊奇, 郑大华, 刘 帅, 于 猛*, 邹忠梅*

(中国医学科学院 北京协和医学院, 药用植物研究所, 道地药材品质保障与资源持续利用全国重点实验室, 北京 100193)

摘要: 研究白芍抗抑郁组分BS-60E在大鼠体内的代谢过程及抑郁状态对其代谢处置的影响。本文复制慢性不可预知温和应激抑郁大鼠模型, 分别灌胃给予正常和抑郁大鼠BS-60E水溶液, 收集血清和尿液样本, 利用UPLC-Q-TOF/MS结合UNIFI软件鉴定原型成分及代谢产物, 并采用多元统计分析方法比较正常与抑郁大鼠体内的差异成分。动物实验均经过中国医学科学院药用植物研究所动物伦理委员会批准 (批准号: SLXD-20211105019)。结果显示, 血清和尿液样本分别检出9个、28个原型成分及33个、60个代谢产物, 主要代谢途径包括羟基化、去饱和等I相反应以及葡萄糖醛酸化、硫酸化等II相反应; 与正常大鼠相比, 芍药苷、1-*O*-*β*-*D*-glucopyranyl paeoniflorone等单萜成分在抑郁大鼠血清和尿液中含量均降低, 而没食子酸甲酯、没食子酸乙酯等多酚类成分在血清中含量降低, 但在尿液中含量升高。以上结果表明, 抑郁状态显著改变了大鼠对BS-60E主要成分的代谢处置, 表现为单萜类成分吸收减少, 血清与尿液中原型成分暴露量降低, 其药效作用可能主要依赖于代谢产物并经肾脏以代谢形式排出; 多酚类成分经肾脏排泄加快, 血清浓度降低而尿中排泄量增加, 其原型成分可能直接参与药效过程, 并以原型及代谢产物形式经尿液排出。

关键词: 白芍; 抗抑郁组分; 单萜; 多酚; 代谢过程

中图分类号: R917 **文献标识码**: A **文章编号**: 0513-4870(2026)07-2682-12

Metabolism of the antidepressant fraction from Bai-Shao in rats and the effect of depression on its disposition

HE Hao-qi, ZHENG Da-hua, LIU Shuai, YU Meng*, ZOU Zhong-mei*

(*State Key Laboratory for Quality Ensurance and Sustainable Use of Dao-di Herbs, Institute of Medicinal Plant Development, Chinese Academy of Medical Sciences & Peking Union Medical College, Beijing 100193, China*)

Abstract: The study aims to investigate the metabolic process of the antidepressant component (BS-60E) from Paeoniae Radix Alba in rats, and to compare the differences in the disposition of its metabolites between normal and depressed states. In this study, a chronic unpredictable mild stress (CUMS) depression model was established in rats. Normal and depressed rats were orally administered the BS-60E aqueous solution, and serum and urine samples were collected. The prototype constituents and metabolites were identified using UPLC-Q-TOF/MS combined with UNIFI software, and multivariate statistical analysis was employed to compare the differential constituents between normal and depressed rats. Animal experimental procedures were approved by the Animal Ethics Committee of the Institute of Medicinal Plant Development, Chinese Academy of Medical Sciences & Peking Union Medical College (approval No.: SLXD-20211105019). The results showed that 9 and 28 prototype constituents, as well as 33 and 60 metabolites, were detected in serum and urine samples, respectively. The main metabolic pathways included phase I reactions such as hydroxylation and desaturation, and phase II reactions

收稿日期: 2026-01-27; 修回日期: 2026-04-14.
基金项目: 国家自然科学基金资助项目 (82073991).
*通讯作者 Tel: 86-10-57833290; E-mail: zmzou@implad.ac.cn; myu@implad.ac.cn
DOI: 10.16438/j.0513-4870.2026-0116

including glucuronidation and sulfation. Compared with normal rats, the levels of monoterpene constituents such as paeoniflorin and 1-*O*-*β*-*D*-glucopyranyl paeoniflorone were decreased in both serum and urine of depressed rats, while the levels of polyphenolic constituents such as methyl gallate and ethyl gallate were decreased in serum but increased in urine. These results indicate that the depressed state significantly alters the metabolic disposition of the main constituents of BS-60E in rats. This is manifested as reduced absorption of monoterpene constituents, leading to decreased exposure of prototype constituents in serum and urine, suggesting that their pharmacological effects may primarily depend on metabolites and are excreted *via* the kidneys in metabolized forms. Meanwhile, the renal excretion of polyphenolic constituents is accelerated, resulting in decreased serum concentrations and increased urinary excretion, suggesting that their prototype constituents may directly participate in the pharmacological process and are excreted in urine both as prototypes and metabolites.

Key words: Paeoniae Radix Alba; antidepressant component; monoterpene; polyphenol; metabolic process

白芍是毛茛科芍药属植物芍药 *Paeonia lactiflora* Pall. 的干燥根, 味苦、酸, 性微寒, 归肝、脾经, 具有养血调经、敛阴止汗、柔肝止痛和平抑肝阳等功效[1], 其化学成分主要包含萜类及其糖苷、多酚、黄酮、有机酸等, 具有抗炎、抗氧化、保肝、抗抑郁、神经保护、抗菌、抗肿瘤以及免疫调节等多种药理活性[2]。近年来, 白芍的抗抑郁作用被逐渐关注[3]。依据用药频次分析和中药组方关联规则, 白芍是临床治疗抑郁症复方中的核心药物之一[4], 可通过多成分、多通路、多靶点发挥抗抑郁疗效。其中芍药苷、芍药内酯苷是白芍中含量较高的单萜类成分, 能通过上调单胺能神经递质水平[5]、抑制下丘脑–垂体–肾上腺轴功能亢进[6]、促进神经保护[7]、抑制炎症反应[8]、下调一氧化氮水平[9]等多种途径改善抑郁症状, 被认为是白芍发挥抗抑郁药效的核心成分。

课题组前期通过皮质酮诱导的 PC12 细胞神经损伤模型结合小鼠行为绝望模型, 证实白芍醇提物大孔树脂洗脱组分 BS-60E 为白芍抗抑郁活性部位, 并从中鉴定出 79 个化学成分[10], 主要包括单萜类和多酚类等成分。然而, 该组分在体内的代谢过程尚不清晰。中药血清药物化学研究发现, 入血成分及其代谢产物对于中药发挥药效至关重要[11]。中药在体内吸收、分布、代谢和排泄受肠道微生物群、转运体、代谢酶活性等多种因素调节[12-14], 而病理状态下体内微环境变化也可能影响成分代谢[15]。已有研究结果显示, 白芍中的单体成分氧化芍药苷在正常与抑郁大鼠体内的代谢存在显著差异[16]。因此, 系统比较 BS-60E, 特别是其中的单萜类和多酚类成分在正常与抑郁状态下的体内代谢过程及产物差异, 对阐明白芍抗抑郁物质基础具有重要意义。

基于此, 本研究采用超高效液相色谱串联四级杆飞行时间质谱 (UPLC-Q-TOF/MS) 技术, 结合 UNIFI 等体内过程分析软件, 全面鉴定与表征 BS-60E 在正常大鼠血清和尿液中的原型成分和代谢产物, 并考察这些原型成分及代谢产物在抑郁状态下的差异, 以期为揭示白芍抗抑郁的药效物质提供依据。

材料与方法

试剂 质谱级甲醇、乙腈、甲酸 (美国 Thermo Fisher 公司), 超纯水 (屈臣氏), 水合氯醛 (美国 Sigma 公司), 生理盐水 (石家庄四药有限公司), 蔗糖 (国药集团化学试剂有限公司)。

仪器 ACQUITY™ UPLC® 超高效液相色谱串联高分辨质谱联用系统 SYNAPT G2 HDMS、96 孔正压提取装置、MassLynx™ 工作站 Version 4.1 (美国 Water 公司); MSA125P-100-DU 型电子分析天平 (德国 SARTORIUS 公司); KQ-500E 型超声振荡仪 (昆山市超声仪器有限公司); Legend Micro17R 低温高速旋转离心机 (美国 Thermo 公司); S0200-230V-EU 微型涡旋混合仪 (美国 Labnet 公司); XR-XG 201 旷场仪器、XR-XX 220 SuperLHt 学习无助实验箱 (上海欣软信息科技有限公司); SIMCA-P 软件 (Umetrics AB, Sweden, versin 13.0)。

实验动物 雄性 Wistar 大鼠, SPF 级, 体质量 180～200 g, 购于维通利华实验动物有限公司, 实验动物生产许可合格证号 SCXK (京) 2017-0020。本研究所涉及的相关动物实验操作均符合中国医学科学院药用植物研究所动物伦理委员会动物实验指导原则 (批准号: SLXD-20211105019)。所有大鼠在动物房中适应性饲养 7 天, 条件为: 温度 20～25 ℃, 湿度 50% ± 10%, 保持 12 h 照明与 12 h 黑暗交替循环, 自由饮水。

白芍组分 (BS-60E) 溶液配制 精密称取 BS-60E 冻干粉 (实验室自制, 制备方法参照文献[10]) 适量, 加入超纯水, 超声辅助溶解, 配制成质量浓度约为 0.28 g·mL^{-1} 的混悬液, 备用。

动物实验分组及给药 选取大鼠 12 只, 随机分为正常给药组 (control, n = 6) 和抑郁模型给药组 (model,

n = 6), 参照文献[17]方法复制慢性不可预知应激抑郁 (chronic unpredictable mild stress, CUMS) 大鼠模型, 通过体重、自主活动、糖水偏好等行为学指标判断造模是否成功; 待造模成功后, 对正常组和抑郁模型组大鼠同时口服给予BS-60E水溶液混悬液, 给药体积10 mL·kg^{-1} (给药剂量2.8 g·kg^{-1}, 按提取物计), 每天1次, 连续3 d。

尿液样本采集与处理 连续给药3 d后, 通过代谢笼收集各组大鼠的尿液样本, 于4 ℃、13 000 r·min^{-1}下离心15 min, 取上清液, 待测。

血清样本采集与处理 连续给药3 d后, 将各组大鼠禁食不禁水12 h, 在末次口服给药BS-60E混悬液1 h后, 使用4%水合氯醛溶液麻醉, 采集各组大鼠腹主动脉全血置于空白采血管中, 在4 ℃、3 500 r·min^{-1}下离心15 min, 取上清液, 即得血清样本。精密移取200 μL各组血清样本加入到Ostro96孔除磷脂板中, 加入3倍体积含1%甲酸的乙腈溶液, 混匀, 采用正压装置对样品进行过滤, 收集滤液, 使用氮气挥干溶剂, 再用50%甲醇100 μL复溶, 保持4 ℃下、13 000 r·min^{-1}离心15 min, 取上清液, 待测。

色谱条件 色谱柱: ACQUITY UPLC HSS T3 (100 mm × 2.1 mm, 1.8 μm); 流动相: 0.1%甲酸水溶液 (A)−0.1%甲酸乙腈 (B); 梯度洗脱程序: 0～4 min, 1%～4% B; 4～6 min, 4%～12% B; 6～16 min, 12%～23% B; 16～18 min, 23%～50% B; 18～20 min, 50%～99% B; 流速: 0.3 mL·min^{-1}; 柱温: 40 ℃; 检测波长: 190～400 nm; 进样量: 5 μL。

质谱条件 采用Waters SYNAPT G2 HDMS系统, 以氮气作为质谱ESI离子源的雾化气和锥孔气; 电喷雾电离, 正负离子模式; 毛细管电压: 2.3 kV; 离子源温度为100 ℃; 脱溶剂气温度为400 ℃; 萃取锥孔电压为3 V; 锥孔电压为40 V; 反向锥孔气流为50 L·h^{-1}; 碰撞气流速为0.5 mL·min^{-1}; 脱溶剂气流速为600 L·h^{-1}; 扫描时间为0.5 s; 扫描时间间隔为0.02 s; 扫描质荷比范围为m/z 50～1 200; 以亮氨酸−脑啡肽溶液作为校正液进行精确质量校正 (锁定质量数: 正离子模式m/z 556.277 1; 负离子模式m/z 554.261 5)。

数据处理 采集各组大鼠血清和尿液样本的质谱数据, 通过MassLynx 4.1软件对所得质谱数据进行预处理, 然后导入到UNIFI软件进行数据分析。利用质谱碎片离子和精确质量数对化合物进行过滤、筛选和鉴定, 以响应强度高于500、质量偏差范围小于10 ppm为条件预测代谢物准分子离子峰。利用MassLynx V 4.1中的MarkerLynx模块对各组大鼠尿液和血清样本所得的质谱数据进行自动归一化、峰识别和噪音过滤等预处理 (处理参数包括: 时间范围、质量范围、质量偏差等), 最后输出由保留时间、质荷比和峰面积组成的数据集。将数据集导入SIMCA-P软件中进行多元化统计分析, 包括主成分分析 (PCA) 和正交偏最小二乘−判别分析 (OPLS-DA), 以OPLS-DA模型中的S-plot加载分析和变量重要性分析 (VIP) 找到区分正常组和抑郁大鼠组间差异的原型成分和代谢产物。

统计学分析 数据组间对比采用IBM SPSS 27.0软件进行独立样本t检验, 运用GraphPad Prism 9.5进行柱形图绘制, 实验数据以平均值 ± 标准差表示 ($\bar{x} \pm s$), $P < 0.05$表示具有统计学意义。

结果

1 行为学特征

慢性应激刺激造模28 d后, 模型大鼠体重 ($P < 0.001$)、运动总距离 ($P < 0.01$) 和蔗糖水消耗 ($P < 0.05$) 均显著低于正常大鼠 (图1), 说明慢性应激抑郁大鼠造模成功, 且模拟了抑郁症患者体重减轻、自主活动减少和食欲减退等症状。

2 BS-60E进入正常大鼠体内成分的鉴定

根据优化的色谱质谱分析条件, 分别采集大鼠含药血清和尿液样本正负离子模式下的质谱数据。经系统比较分析, 结合课题组前期对BS-60E化学成分鉴定的结果[10], BS-60E中的主要成分在负离子模式下具有

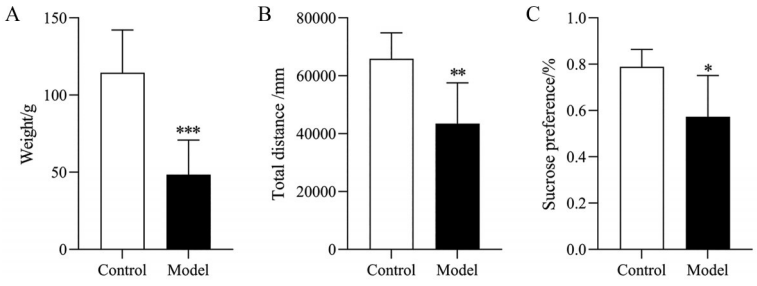


Figure 1 Comparison of weight change (A), total distance traveled in the open field test (B), and sucrose preference (C) between the normal group rats and the depression model group rats. Control: Normal group; Model: Chronic unpredictable mild stress (CUMS) model group; n = 6, $\bar{x} \pm s$. $^{*}P < 0.05$; $^{**}P < 0.01$; $^{***}P < 0.001$ *vs* control

更高的信号响应强度和分辨率, 更适合后续分析。因此, 本论文仅选取负离子模式下的质谱数据 (图2) 进行深入分析 (正离子模式质谱图略)。接着, 将BS-60E中所鉴定的化学成分信息 (分子式, *m*/*z*) 导入UNIFI软件中作为母体化合物, 与空白样本对比扣除杂质信号干扰, 参照可能的体内代谢产物加合离子信息, 根据碎片离子信息、响应度、准确度、理论碎片等代谢产物数据, 分别对大鼠血清和尿液样本中的BS-60E原型成分和代谢产物进行鉴定。原型成分 (C0、D0、L0、O0、P0、Q0、S0、Z0) 和12个代谢产物 (B4、G3、K2、K4、L1、L6、Q3、Q4、Q5、U2、III5、III6) 在血清和尿液中均检测到, 鉴定结果见表1。

此外, 在正常大鼠血清样本中, 1-*O*-*β*-*D*-glucopyranosyl paeonisuffrone (D0)、二没食子酰葡萄糖 (F0)、苯甲酰芍药苷 (Z0) 等3个成分仅检测到其原型成分; 单宁酸 (B4)、6-*O*-glucopyranoglucoside (G3)、牡丹皮苷F (H2)、儿茶素 (J1)、catechin glucoside (K1～K4)、glucosylpaeoniflorin (N1)、galloylpaeoniflorin (T2)、牡丹皮苷I (U2～U4)、pinen-10-yl-*β*-vicianoside (II7)、牡丹皮苷E (III2、III5、III6)、paeonimetabolin I (IV1、IV2) 等19个化学成分仅检测到代谢产物; 没食子酰葡萄糖 (C0)、氧化芍药苷 (L0)、芍药内酯苷 (O0)、芍药苷 (P0)、没食子酸乙酯 (Q0)、四没食子酰葡萄糖 (S0) 等6个化学成分同时检测到原型成分及代谢产物。

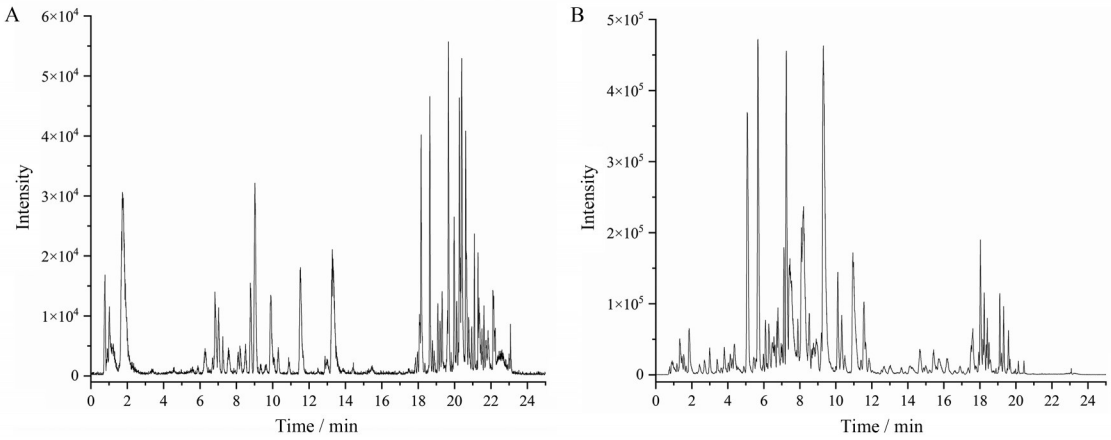


Figure 2 The base peak ion (BPI) chromatogram in negative ion mode of serum (A) and urine (B) samples from normal rats after oral administration of BS-60E

Table 1 Identification prototype and metabolite results of BS-60E in rats (+: The sample source of metabolites; /: No metabolites were detected). U: Urine; S: Serum; SN: Serial number

No.	SN	t_R/min	Prototype composition	Metabolic pathway	Structural formula	*m*/*z*	Negative ion fragment	Error (ppm)	Source	
									U	S
1	A0	2.86	Desbenzoylpaeoniflorin	Parent	$C_{16}H_{24}O_{10}$	375.131 2	165	5.6	+	/
2	A1	2.43		Sulfation	$C_{16}H_{24}O_{13}S$	456.093 8	275, 345	10	+	/
3	B0	4.74	Galloylglucose	Parent	$C_{13}H_{16}O_{10}$	331.066 1	125, 211	−1.3	+	/
4	B1	3.25		Glycoside hydrolysis+glucuronidation	$C_{13}H_{14}O_{11}$	345.044 0	125, 169	−6.9	+	/
5	B2	3.83		Glycoside hydrolysis+glucuronidation+glucuronidation	$C_{19}H_{22}O_{17}$	521.076 8	169, 246	−3.1	+	/
6	B3	3.97		Reduction	$C_{13}H_{18}O_{10}$	333.080 9	125	−5.8	+	/
7	B4	4.34		Glycoside hydrolysis+glucuronidation+decarboxylation	$C_{12}H_{14}O_9$	301.054 0	125, 204, 301	−8.6	+	+
8	B5	4.6		Glucuronidation	$C_{19}H_{24}O_{16}$	507.095 2	331	−7.9	+	/
9	C0	5.71	Galloylsucrose	Parent	$C_{19}H_{26}O_{15}$	493.124 4	137, 211	9.1	+	+
10	C1	4.58		Hydroxylation	$C_{19}H_{24}O_{16}$	507.098 6	445	−0.1	+	/
11	C2	4.70		Hydroxylation+desaturation+methylation	$C_{20}H_{26}O_{16}$	521.115 0	124, 168, 183	0.2	/	+
12	C3	6.97		Hydroxylation+acetylization	$C_{21}H_{26}O_{17}$	549.112 2	197, 261, 373	5.5	+	/
13	D0	4.21	1-*O*-*β*-*D*-Glucopyranosyl	Parent	$C_{16}H_{24}O_9$	359.132 3	179, 197	−5.3	+	+
14	D1	2.34	paeonisuffrone	3×Hydroxylation	$C_{16}H_{22}O_{12}$	405.107 1	405	9.3	+	/
15	D2	4.16		Hydroxylation+desaturation	$C_{16}H_{22}O_{10}$	373.110 2	315, 359	−8.8	+	/
16	D3	5.22		Desaturation	$C_{16}H_{22}O_9$	357.116 5	233	−7.1	+	/
17	E0	6.03	Procyanidin C	Parent	$C_{45}H_{38}O_{18}$	865.195 5	243, 407, 695	−3.5	+	/
18	F0	6.59	Digalloylglucose	Parent	$C_{20}H_{20}O_{14}$	483.081 2	151	6.6	/	+
19	F1	7.20		3×Hydroxylation+demethylation	$C_{21}H_{22}O_{17}$	545.076 8	444, 511	−2	+	/

Continued

No.	SN	t_R/min	Prototype composition	Metabolic pathway	Structural formula	*m*/*z*	Negative ion fragment	Error (ppm)	Source	
									U	S
20	G0	6.68	6-*O*-	Parent	$C_{16}H_{26}O_9$	361.151 6	355	4.7	+	/
21	G1	1.09	Glucopyranoglucoside	-$C_{10}H_{14}O_4$+reduction+glucuronide conjugation	$C_{12}H_{22}O_{11}$	341.108 6	119	−1	+	/
22	G2	3.74		Hydroxylation+desaturation	$C_{16}H_{24}O_{10}$	375.126 0	376	−8.4	+	/
23	G3	4.83		Hydroxylation	$C_{16}H_{26}O_{10}$	377.144 4	113, 359	−2.4	+	+
24	H0	6.79		Parent	$C_{16}H_{24}O_8$	343.139 2	292	−0.3	+	/
25	H1	3.77	Mudanpioside F	Hydroxylation+desaturation	$C_{16}H_{22}O_9$	357.118 6	357	0	+	/
26	H2	7.28		Hydroxylation	$C_{16}H_{24}O_9$	359.134 7	348	1.3	/	+
27	H3	8.93		Reduction+acetylization	$C_{18}H_{28}O_9$	387.164 9	387	−1.6	+	/
28	I0	6.94	Strictinin	Parent	$C_{27}H_{22}O_{18}$	633.072 9	152, 300	−0.8	+	/
29	J0	7.04	Catechin	Parent	$C_{15}H_{14}O_6$	289.074 4	121, 125	10.0	+	/
30	J1	7.05		Glucuronide conjugation	$C_{21}H_{22}O_{12}$	465.107 7	123, 289	8.2	/	+
31	K0	7.20	Catechin glucoside	Parent	$C_{21}H_{24}O_{11}$	451.124 6	137, 289, 311	0.1	+	/
32	K1	6.47		Hydroxylation+desaturation	$C_{21}H_{22}O_{12}$	465.107 0	108, 123, 152	6.7	/	+
33	K2	7.54		Hydroxylation+desaturation+methylation	$C_{22}H_{24}O_{12}$	479.122 2	122, 137, 303	5.4	+	+
34	K3	7.93		Hydration+acetylization	$C_{23}H_{28}O_{13}$	511.143 5	169	−4.5	+	/
35	K4	11.55		Dehydration	$C_{21}H_{22}O_{10}$	433.111 6	151, 271	−5.4	+	+
36	L0	7.81	Oxypaeoniflorin	Parent	$C_{23}H_{28}O_{12}$	495.149 8	165, 177	−1.0	+	+
37	L1	4.98		-$C_7H_4O_3$+hydration	$C_{16}H_{26}O_{10}$	377.144 7	113	−1.7	+	+
38	L2	5.96		-$C_7H_4O_3$+hydration+reduction	$C_{16}H_{28}O_{10}$	379.158 4	375	−7.0	+	/
39	L3	6.38		Glucuronide conjugation	$C_{29}H_{36}O_{18}$	671.180 6	160, 265	−3.5	+	/
40	L4	6.53		-$C_7H_4O_2$+reduction	$C_{16}H_{26}O_{10}$	377.148 0	113, 359	6.9	/	+
41	L5	7.41		Glucosylation	$C_{29}H_{38}O_{17}$	657.203 4	137, 177	−0.3	+	/
42	L6	8.03		-$C_7H_4O_3$+2×hydroxylation+desaturation+sulfation	$C_{16}H_{20}O_{14}S$	467.053 7	183, 196, 359	7.7	+	+
43	L7	8.32		Deglucose+hydroxylation+desaturation+hydroxylation+acetylization	$C_{19}H_{18}O_{10}$	405.081 0	207, 273	−4.3	/	+
44	L8	8.39		-$C_7H_4O_3$+reduction	$C_{16}H_{26}O_9$	361.153 3	113, 301	7.8	+	/
45	L9	10.74		Decarboxylation+desaturation	$C_{22}H_{26}O_{10}$	449.143 5	446	−4.0	+	/
46	M0	9.04	Diglucopaeoniflorin	Parent	$C_{35}H_{48}O_{21}$	803.264 1	121, 179, 383	3.2	+	/
47	M1	11.84		-$C_{12}H_{20}O_{10}$+desaturation+glucuronide conjugation	$C_{29}H_{34}O_{17}$	653.167 7	111, 475, 543	−7.0	+	/
48	N0	9.33	Glucosylpaeoniflorin	Parent	$C_{29}H_{38}O_{16}$	641.211 7	121, 165, 489	5.5	+	/
49	N1	17.44		Deglucose+decarboxylation+hydration	$C_{22}H_{30}O_{10}$	453.175 3	149, 219	−3.2	/	+
50	O0	9.64	Albiflorin	Parent	$C_{23}H_{28}O_{11}$	479.155 0	123, 196, 370	3.2	+	+
51	O1	5.57		-$C_7H_4O_2$+hydration	$C_{16}H_{26}O_{10}$	377.147 0	113, 133, 359	4.4	/	+
52	O2	6.89		-C_7H_4O+hydroxylation	$C_{16}H_{24}O_{12}$	407.122 2	181, 203, 373	6.6	/	+
53	O3	7.36		-C_7H_4O+glycoside hydrolysis+glucuronidation+-H_2O	$C_{16}H_{20}O_{10}$	371.101 2	146	7.7	/	+
54	O4	8.14		-C_7H_4O+oxidation+-CO	$C_{16}H_{26}O_9$	361.152 8	121, 175	6.4	+	/
55	O5	15.31		-C_7H_4O+oxidation+decarboxiylic	$C_{16}H_{26}O_8$	345.155 6	164	0.1	/	+
56	P0	10.28	Paeoniflorin	Parent	$C_{23}H_{28}O_{11}$	479.155 0	121, 196, 211	3.2	+	+
57	P1	8.52		Demethylation+hydroxylation	$C_{22}H_{24}O_{12}$	479.111 6	479	−4.9	+	/
58	P2	9.39		Glucosylation	$C_{29}H_{38}O_{16}$	687.219 1	121, 211, 409	7.3	/	+
59	P3	10.31		Oxidation+decarboxylic	$C_{22}H_{26}O_{10}$	449.141 5	449	−7.4	/	+
60	Q0	10.54	Ethyl gallate	Parent	$C_9H_{10}O_5$	197.046 8	124	9.1	+	+
61	Q1	4.48		-C_2H_4+sulfation	$C_7H_6O_8S$	248.968 7	125, 169	−9.4	+	/
62	Q2	5.47		-C_2H_4+glucuronidation	$C_{13}H_{14}O_{11}$	345.043 8	125, 169	−7.3	+	/
63	Q3	6.18		Demethylation+sulfation	$C_8H_8O_8S$	262.987 2	168, 183	3.8	+	+
64	Q4	8.45		Glucuronidation	$C_{15}H_{18}O_{11}$	373.080 6	124, 197	7.9	+	+
65	Q5	9.97		Sulfation	$C_9H_{10}O_8S$	277.002 0	124, 197	0.6	+	+
66	Q6	10.69		-C_2H_4+glucuronidation+-H_2O	$C_{15}H_{20}O_8$	327.107 7	121	−2.7	+	/
67	R1	5.40	Methyl gallate	Decarboxylation+sulfation	$C_7H_8O_6S$	218.995 0	109, 138, 188	−8.5	+	/
68	S0	11.39	Tetragalloylglucose	Parent	$C_{34}H_{28}O_{22}$	787.101 5	123, 195, 409	1.9	+	+
69	S1	11.01		3×Hydroxylation+sulfation	$C_{34}H_{28}O_{28}S$	915.037 6	897	−3.7	/	+
70	T0	12.99	Malloylpaeoniflorin	Parent	$C_{30}H_{32}O_{15}$	631.167 2	121, 160	1.4	+	/
71	T1	8.29		Reduction+demethylation+decarboxylation+glucuronide conjugation	$C_{34}H_{40}O_{20}$	767.208 6	628	6.6	+	/
72	T2	10.11		2×Hydroxylation+demethylation+decarboxylation+glucuronide conjugation	$C_{34}H_{38}O_{22}$	797.179 4	659, 797	2.2	/	+
73	T3	11.25		Glucuronide conjugation	$C_{36}H_{40}O_{21}$	807.197 5	613, 631	−1.8	+	/

Continued

No.	SN	t_R/min	Prototype composition	Metabolic pathway	Structural formula	*m/z*	Negative ion fragment	Error (ppm)	Source	
									U	S
74	U0	15.54	Mudanpioside I	Parent	$C_{23}H_{28}O_{11}$	479.155 0	121, 331	3.2	+	/
75	U1	8.60		Glucosylation	$C_{29}H_{38}O_{16}$	687.216 1	121, 489	2.9	+	/
76	U2	11.44		-$C_{13}H_{14}O_6$+desaturation+sulfation	$C_{10}H_{12}O_8S$	291.017 3	123, 166, 196	−2.1	+	+
77	U3	11.87		Reduction+demethylation+sulfation	$C_{22}H_{28}O_{14}S$	547.116 3	485, 547	7.5	/	+
78	U4	12.87		-$C_{13}H_{14}O_7$+hydroxylation+desaturation+sulfation	$C_{10}H_{12}O_8S$	291.019 9	123, 166, 196	6.5	/	+
79	W0	12.38	Mudanpioside H	Hydroxylation+glucosylation	$C_{36}H_{42}O_{20}$	793.215 5	433, 491, 613	−5.2	+	/
80	X0	16.99	Digalloylpaeoniflorin	Parent	$C_{37}H_{36}O_{19}$	783.172 9	183, 465, 631	−6.2	+	/
81	Y0	17.90	Benzoyloxypaeoniflorin	Parent	$C_{30}H_{32}O_{13}$	599.178 3	137	2.2	+	/
82	Y2	18.36		-$C_7H_4O_2$+decarboxylation+glucosylation	$C_{28}H_{38}O_{14}$	597.218 8	283, 445	−0.1	+	/
83	Z0	18.54	Benzoylpaeoniflorin	Parent	$C_{30}H_{32}O_{12}$	583.183 1	121, 217, 449	1.8	+	+
84	Z1	12.38		Hydration+hydroxylation+glucuronide conjugation	$C_{36}H_{42}O_{20}$	793.215 5	433, 491, 613	−5.3	+	/
85	Z2	17.53		2×Hydroxylation	$C_{30}H_{32}O_{14}$	615.172 2	169, 217	0.6	+	/
86	Z3	17.97		Glucosylation	$C_{36}H_{42}O_{17}$	745.234 3	169, 313	−0.8	+	/
87	I0	7.34	Procyanidin C	Parent	$C_{30}H_{26}O_{12}$	577.135 3	125, 289	0.2	+	/
88	II0	18.05	(*Z*)-(1*S*,5*R*)-*β*-Pinen-10-yl-*β*-vicianoside	Parent	$C_{21}H_{34}O_{10}$	445.205 7	137	−3.8	+	/
89	II1	7.71		-$C_{11}H_{18}O_9$+2×hydroxylation+glucuronide conjugation	$C_{16}H_{24}O_9$	359.137 7	123	8.3	+	/
90	II2	15.95		-$C_5H_8O_4$+2×desaturation+sulfation	$C_{16}H_{22}O_9S$	389.089 5	235	−4.1	+	/
91	II3	17.78		Reduction	$C_{21}H_{36}O_{10}$	447.222 6	101, 161, 315	−2.2	+	/
92	II4	18.00		Reduction+methylation	$C_{22}H_{38}O_{10}$	461.238 2	121, 177, 327	−2.4	+	/
93	II5	9.36		-$C_{11}H_{18}O_9$+hydration+hydroxylation+glucuronide conjugation	$C_{16}H_{26}O_9$	361.148 4	113, 268	−5.6	+	/
94	II6	9.80		-$C_5H_8O_4$+hydroxylation+desaturation+acetylization	$C_{18}H_{26}O_8$	369.158 6	124, 197	8.2	+	/
95	II7	7.10		2×Hydroxylation+demethylation+sulfation+glutathione conjugation	$C_{30}H_{47}N_3O_{21}S_2$	848.205 2	535, 826	−1.6	/	+
96	III0	8.34	Mudanpioside E	Parent	$C_{24}H_{30}O_{13}$	525.166 0	167, 359, 383	8.8	+	/
97	III1	5.32		-$C_{16}H_{22}O_9$+hydroxylation+glucuronide conjugation	$C_{14}H_{16}O_{11}$	359.059 5	168	−6.9	+	/
98	III2	6.69		-CH_2O+2×decarboxylation	$C_{21}H_{28}O_8$	407.173 7	203, 239	6.2	/	+
99	III3	7.29		Decarboxylation+dehydrate+sulfation	$C_{23}H_{28}O_{13}S$	543.122 7	132, 212, 446	9.1	+	/
100	III4	8.22		Demethylation	$C_{23}H_{28}O_{13}$	511.146 2	169	0.9	+	/
101	III5	8.77		3×Hydroxylation+glucuronide conjugation	$C_{30}H_{36}O_{22}$	747.161 7	747	−0.4	+	+
102	III6	10.86		Hydroxylation+desaturation+decarboxylation	$C_{23}H_{28}O_{12}$	495.148 8	137, 345	−4.1	+	+
103	III7	11.03		Decarboxylation+hydroxylation	$C_{23}H_{30}O_{12}$	497.163 6	169, 271	−5.7	+	/
104	IV1	8.80	Paeonimetabolin I	Glucuronide conjugation	$C_{15}H_{18}O_{11}$	373.075 2	197	−5.1	/	+
105	IV2	6.95		2×Glucuronide conjugation	$C_{22}H_{30}O_{16}$	549.146 9	549	2.4	/	+

2.1 单萜类化合物代谢产物的鉴定 以芍药内酯苷($C_{23}H_{28}O_{11}$, O0)和芍药苷($C_{23}H_{28}O_{11}$, P0)为例。正常大鼠口服BS-60E后检测到芍药内酯苷原型成分和5个代谢产物(O1～O5), 除O4存在于尿液中外, 其他4个代谢产物(O1～O3、O5)存在于血清中; 正常大鼠血清和尿液样本中鉴定到芍药苷原型成分和3个代谢产物(P1～P3), 其中P2和P3两个代谢产物存在于血清中, P1存在于尿液中。推测的代谢途径见图3。

O1的准分子离子峰*m/z* 377.147 0 ($[M-H]^-$), 通过元素组成推测其分子式为$C_{16}H_{26}O_{10}$(*m/z* 378.152 6)比原型成分少102 Da, 推测可能为芍药内酯苷脱去1分子苯甲酸($C_7H_4O_2$)后发生水合反应产生的代谢产物; O2的准分子离子峰*m/z* 407.122 2 ($[M-H]^-$, $C_{16}H_{23}O_{12}$), 比原型成分少72 Da, 推测其可能由芍药内酯苷脱去1分子C_7H_4O后发生两次羟基化反应产生; O3的准分子离子峰*m/z* 371.101 2 ($[M-H]^-$, $C_{16}H_{20}O_{10}$), 推测由芍药内酯苷脱除1分子C_7H_4O后, 葡萄糖基转变为葡萄糖醛酸基后发生一系列复杂代谢过程丢失1分子H_2O而产生的代谢物; O4、O5推测为芍药内酯苷脱除1分子C_7H_4O所形成的羟甲基, 再经氧化脱除CO或羧基形成的代谢产物。P1的准分子离子峰*m/z* 479.111 6 ($[M-H]^-$), 通过元素组成推测分子式为$C_{22}H_{24}O_{12}$, 参照体内可能发生的代谢反应, 推测其为芍药苷羟基化及去甲基化后的代谢产物; P2的准分子离子峰*m/z* 687.219 1 ($[M+HCOO]^-$), 比原型芍药苷增加208 Da, 可能为芍药苷发生葡萄糖基化反应产生的代谢产物, 推测分子式为

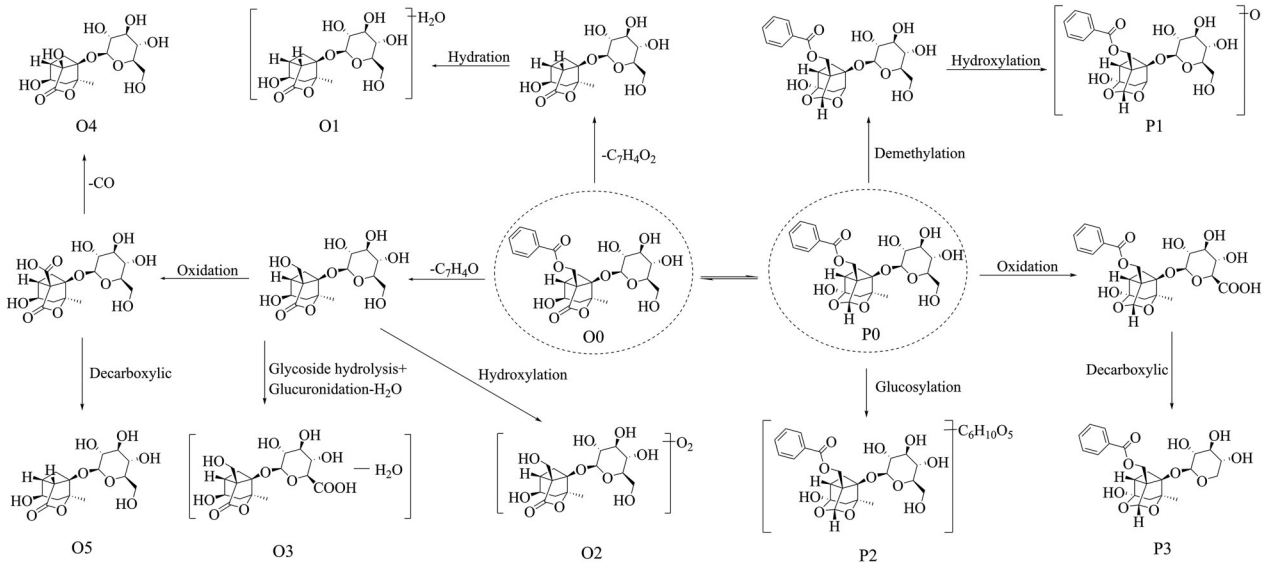


Figure 3 Metabolic pathways of albiflorin and paeoniflorin

$C_{29}H_{38}O_{16}$; P3 的准分子离子峰 *m*/*z* 449.141 5 ([M−H]$^-$), 推测的分子式为 $C_{22}H_{26}O_{10}$, 与原型相差 30 Da, 可能为芍药苷葡萄糖基化后 6 位羟基氧化后脱羧产生的代谢产物。

2.2 多酚类化合物代谢产物的鉴定 以没食子酸乙酯 ($C_9H_{10}O_5$, Q0) 为例, 其原型成分在血清和尿液中均被检测到, 在尿液中鉴定到 6 个代谢产物 (Q1～Q6), 但在血清中只观察到 Q3～Q5 3 个代谢产物。Q1、Q2 均含有原型化合物没食子酸乙酯的特征离子碎片 *m*/*z* 125、169, 且其准分子离子峰 *m*/*z* 248.968 7 ([M−H]$^-$, $C_7H_6O_8S$) 和 *m*/*z* 345.043 8 ([M−H]$^-$, $C_{13}H_{14}O_{11}$) 比原型分别增加了 51 和 148 Da, 推测为其原型成分脱去乙烯基后分别发生硫酸化和葡萄糖醛酸化反应产生的代谢产物; Q3 原型成分通过去甲基化以及硫酸化反应产生; Q4、Q5 与原型相比, 准分子离子峰 *m*/*z* 373.080 6 ([M−H]$^-$, $C_{15}H_{18}O_{11}$)、*m*/*z* 277.002 0 ([M−H]$^-$, $C_9H_{10}O_8S$), 分别增加了 176 和 79 Da, 为原型葡萄糖醛酸化及硫酸化的代谢产物; Q6 则是在 Q2 的基础上继续失去一分子 H_2O 后的代谢产物。推测代谢途径如图 4 所示。

儿茶素葡萄糖 ($C_{21}H_{24}O_{11}$, K0): 原型成分仅在尿液中发现, K1、K2 等 2 个代谢产物存在于血清中, K2～K4 等 3 个代谢产物存在于尿液中, 主要代谢途径有氧化去饱和、水合等, 代谢途径见图 5; 没食子酸葡萄糖 ($C_{13}H_{16}O_{10}$, B0): 原型成分仅在尿液中发现, 5 个代谢产

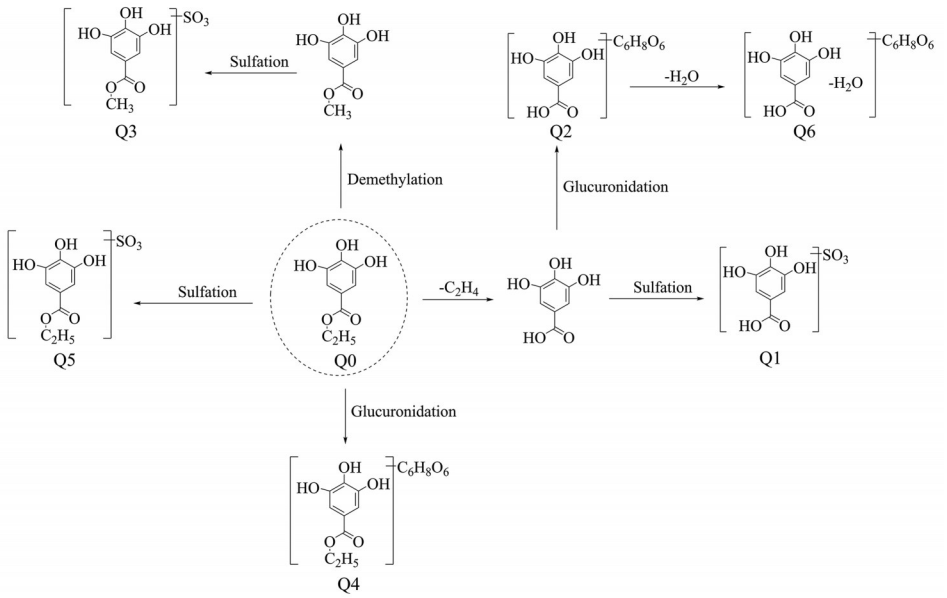


Figure 4 Metabolic pathway of ethyl gallate

物B1～B5等均在尿液中检测到, 但血清中仅观察到代谢产物B4, 主要代谢途径有羟基化、葡萄糖醛酸化、去饱和等, 推测代谢途径见图6。

3 抑郁大鼠对BS-60E入血成分的影响

采用与正常大鼠血清样本相同的前处理及色谱质谱分析方法, 检测抑郁大鼠血清样本。方法学考察选择QC样本中6个特征离子的保留时间、质荷比进行重复性和稳定考察, 其中重复性的RSD变化范围分别为0.047%～0.595%、0.002%～0.004%, 稳定性的RSD变化范围分别为0.451%～1.539%、0.000%～0.065%, 表明该方法重复性及稳定性良好。通过多元统计分析方法比较BS-60E成分在抑郁与正常大鼠血清中的代谢差异。结果如图7A所示, PCA聚类分析结果显示, 抑郁大鼠与正常大鼠含药血清的代谢轮廓差异明显。对数据进行有监督的OPLS-DA模式识别分析 (图7C, $R^2X = 0.653$、$R^2Y = 1$、$Q^2 = 0.673$), 置换检验 (图7E, $n = 200$) 结果表明模型稳定可靠, 且不存在过拟合情况。采用*S*-plot加载分析 (图7G), 利用VIP > 1筛选两组血清样本的差异成分, 排除内源性成分干扰后, 鉴定出11个差异成分, 其中原型成分2个 (D0、Q0)、代谢产物9个 (J1、K4、P3、Q4、Q5、U2、U4、IV1、IV2, 表2)。与正常大鼠相比, 抑郁大鼠血清中单萜类成分D0、P3、U2、U4、IV1的含量降低, 其中, D0 ($P < 0.05$)、Q4 ($P < 0.01$)、IV1 ($P < 0.01$) 具有显著性差异; 多酚类成分Q0、Q4的含量也显著降低 (图8)。

4 抑郁大鼠对BS-60E进入体内经尿液排泄成分的影响

采集抑郁大鼠尿液样本质谱数据, 比较BS-60E成分在抑郁与正常大鼠尿液中的代谢差异。方法学考察选择QC样本中6个特征离子的保留时间、质荷比进行重复性和稳定考察, 其中重复性的RSD变化范围分别为0.067%～0.522%、0.002%～0.004%, 稳定性的RSD变化范围分别为0.477%～1.032%、0.001%～0.032%, 表明该方法重复性及稳定性良好。PCA聚类分析结果显示 (图7B), 抑郁大鼠和正常大鼠含药尿液中的代谢轮廓差异显著。对数据进行有监督的OPLS-DA模式识别分析 (图7D, $R^2X = 0.781$、$R^2Y = 1$、$Q^2 = 0.976$), 置换检验 (图7F, $n = 200$) 结果表明模型稳定可靠, 无过拟合风险。经*S*-plot加载分析 (图7H), 利用VIP > 1筛选两组尿液样本的差异成分, 排除内源性成分干扰后, 共鉴定出15个差异成分, 其中原型成分3个 (D0、J0、Q0)、代谢产物12个 (C3、D2、D3、G2、H1、J1、K4、L1、L2、R1、II1、II2, 表2)。与正常大鼠相比, 抑郁大鼠尿液样本中单萜类原型成分D0及代谢产物L1的含量

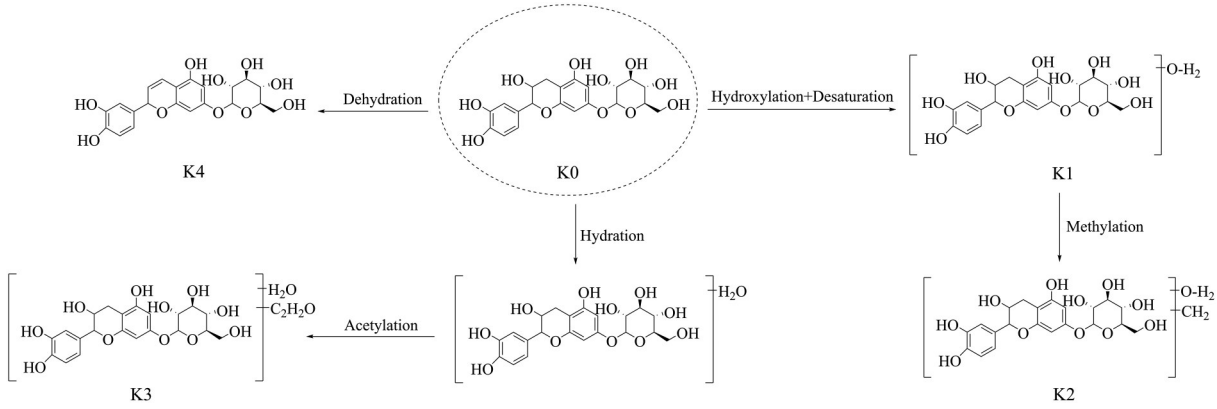


Figure 5 Metabolic pathway of catechin glucoside

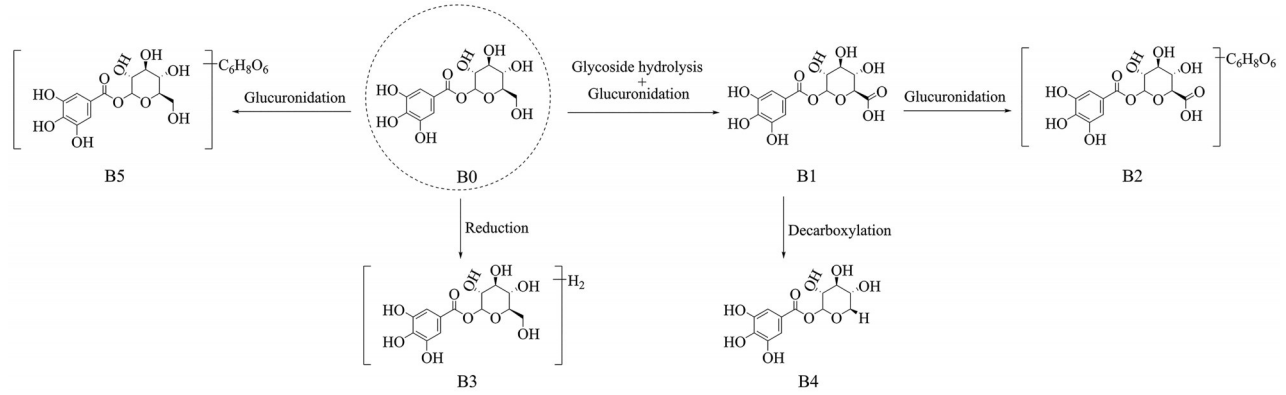


Figure 6 Metabolic pathway of galloylglucose

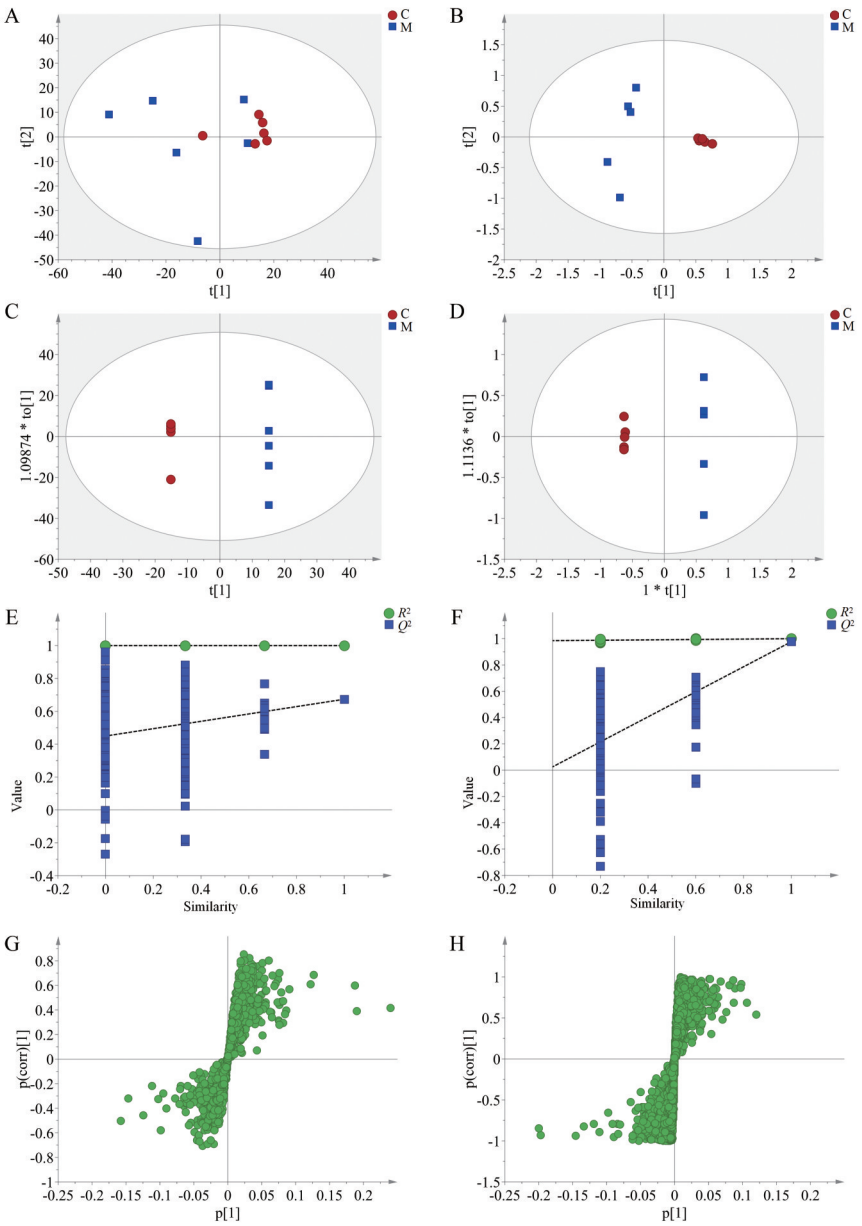


Figure 7 Principal component analysis (PCA, A and B), orthogonal projections to latent structures discriminant analysis (OPLS-DA, C and D), permutation analysis (n = 200, E and F) and the S-plot (G and H) of serum and urine samples from normal and depressed rats. A, C, E, and G: Serum samples of rats; B, D, F, and H: Urine samples of rats

明显升高, 代谢产物D2、D3、H1 ($P < 0.05$) 等的含量明显降低, L2、G2只存在于抑郁大鼠尿液样本中; 多酚类原型成分J0的含量明显升高, Q0的含量显著降低, 代谢产物K4 ($P < 0.01$)、R1等的含量明显升高, C3、J1等代谢产物仅存在于抑郁组中; 其他类代谢产物II1、II2等的含量明显升高 (图9)。

讨论

中药方剂经煎煮口服后发挥作用, 其中可吸收入血的成分或代谢产物被认为是其发挥药效的直接物质基础[18]。在病理状态下, 机体内环境发生紊乱, 对药物的吸收、分布、代谢和排泄过程会产生显著影响, 从而导致与正常生理状态不同的代谢处置差异。阐明这种差异, 对于揭示中药的药效物质基础及作用机制具有重要意义。本研究以“BS-60E”为研究对象, 通过建立抑郁大鼠模型, 采用UPLC-Q-TOF/MS技术, 结合多元统计分析方法, 系统比较BS-60E在正常和抑郁大鼠体内的代谢过程差异。结果发现, 抑郁状态下BS-60E在大鼠体内的代谢过程发生显著改变, 其主要的单萜和多酚类原型成分及代谢产物在抑郁大鼠血清中的含量

Table 2 Comparison of differential constituents of BS-60E in depressed and normal rats

No.	SN	t_R /min	Prototype composition	Metabolic pathway	Structural formula	*m/z*	Error /ppm	VIP vaule	Source U	Source S
1	C3	5.03	Galloylsucrose	Hydroxylation+acetylization	$C_{21}H_{26}O_{17}$	549.109 6	0.7	1.26	+	/
2	D0	4.30	1-*O*-*β*-*D*-Glucopyranyl	Parent	$C_{16}H_{24}O_9$	359.136 4	6.1	2.62	+	+
3	D2	6.94	paeoniflorone	Hydroxylation+desaturation	$C_{16}H_{22}O_{10}$	373.113 5	−4.0	1.14	+	/
4	D3	8.13		Desaturation	$C_{16}H_{22}O_9$	357.118 4	−0.6	1.77	+	/
5	G2	5.32	6-*O*-Glucopyranoglucoside	Hydroxylation+desaturation	$C_{16}H_{24}O_{10}$	375.127 9	−3.2	1.45	+	/
6	H1	3.77	Mudanpioside F	Hydroxylation+desaturation	$C_{16}H_{22}O_9$	357.121 7	8.7	2.06	+	/
7	J0	7.09	Catechin	Parent	$C_{15}H_{14}O_6$	289.072 2	3.5	1.63	+	/
8	J1	7.04		Glucuronide conjugation	$C_{21}H_{22}O_{12}$	465.102 2	−2.4	1.79	+	+
9	K4	17.85	Catechin glucoside	Dehydration	$C_{21}H_{22}O_{10}$	433.111 6	−4.4	1.36	+	+
10	L1	6.84	Oxypaeoniflorin	-$C_7H_4O_4$+reduction	$C_{16}H_{26}O_{10}$	377.145 3	1.3	1.30	+	/
11	L2	6.02		-$C_7H_4O_3$+hydration+reduction	$C_{16}H_{28}O_{10}$	379.158 0	−6.3	3.15	+	/
12	P3	10.31	Paeoniflorin	Oxidation+decarboxylic	$C_{22}H_{26}O_{10}$	449.141 5	−7.4	1.64	/	+
13	Q0	10.61	Ethyl gallate	Parent	$C_9H_{10}O_5$	197.046 0	5.1	2.77	+	+
14	Q4	8.45		Glucuronidation	$C_{15}H_{18}O_{11}$	373.073 7	−9.1	1.28	/	+
15	Q5	9.97		Sulfation	$C_9H_{10}O_8S$	277.001 0	−2.9	1.47	/	+
16	R1	3.68	Methyl gallate	Decarboxylation+sulfation	$C_7H_8O_6S$	218.997 7	6.9	1.83	+	/
17	U2	11.54	Mudanpioside I	-$C_{13}H_{14}O_6$+desaturation+sulfation	$C_{10}H_{12}O_8S$	291.016 8	−2.4	3.43	/	+
18	U4	12.98		-$C_{13}H_{14}O_7$+hydroxylation+desaturation+sulfation	$C_{10}H_{12}O_8S$	291.015 3	−7.6	1.50	/	+
19	II1	5.70	(*Z*)-(1*S*,5*R*)-*β*-Pinen-10-	-$C_{11}H_{18}O_9$+2×hydroxylation+glucuronide conjugation	$C_{16}H_{24}O_9$	359.137 4	8.9	7.00	+	/
20	II2	16.14	yl-*β*-vicianoside	-$C_5H_8O_4$+2×desaturation+sulfation	$C_{16}H_{22}O_9S$	389.089 8	−2.1	3.00	+	/
21	IV1	8.80	Paeonimetabolin I	Glucuronide conjugation	$C_{15}H_{18}O_{11}$	373.075 2	−5.1	2.08	/	+
22	IV2	6.95		2×Glucuronide conjugation	$C_{22}H_{30}O_{16}$	549.146 9	2.4	1.02	/	+

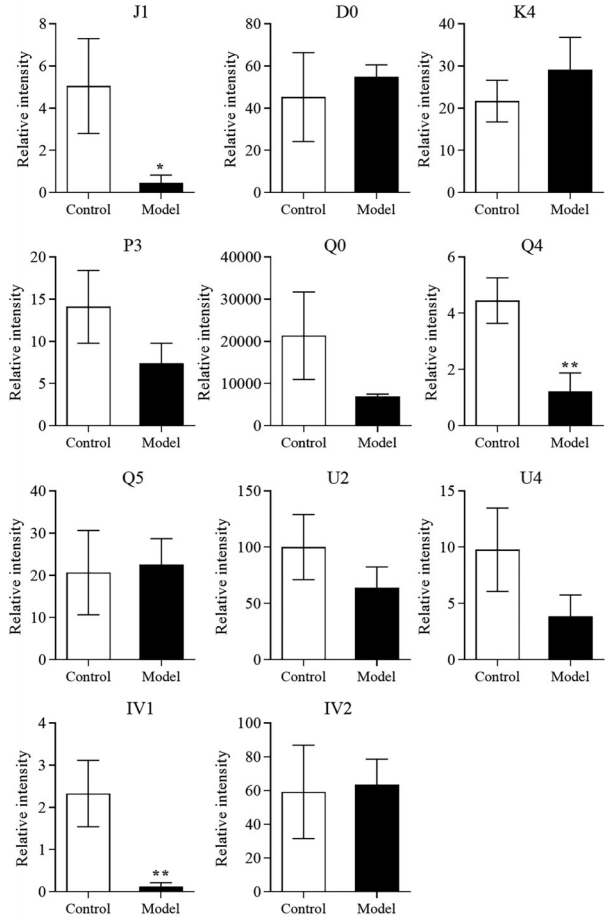


Figure 8 Comparison of the relative contents of differential constituents in serum of normal rats and depressed rats after oral administration of BS-60E. $n = 6$, $\bar{x} \pm s$. $^*P < 0.05$, $^{**}P < 0.01$ *vs* control

低于正常大鼠, 而单萜类成分在尿液中的含量较正常大鼠高。由此推测, BS-60E 中的单萜类成分主要通过其代谢产物发挥药效, 而多酚类成分则可能以原型形式直接参与药效过程, 并以原型及代谢产物形式经尿液排泄。

检测到的入血成分中, 单萜类成分主要以代谢产物的形式存在。单萜类成分的代谢产物均发生了苯甲酰基团脱除, 例如: 氧化芍药苷的代谢产物 L1、L2、L4、L6、L8 脱去对羟基苯甲酰基 (-$C_7H_4O_2$), 芍药内酯苷代谢产物 O1～O5 脱去苯甲酰基。已有研究证实, 氧化芍药苷[19]、芍药苷[20,21]、芍药内酯苷[22]等可通过抑制氧化应激和神经炎症等发挥抗抑郁活性; 苯甲酰芍药苷[23]被报道可显著上调 Nrf2/HO-1 的水平进而调控氧化应激; 没食子酰芍药苷可通过下调 CGRP、TNF-*α*、IL-1*β* 和 IL-18 水平抑制神经源性炎症[24], 同时还可通过激活 PI3K/Akt//Nrf2 通路减轻大鼠氧化应激水平和炎症反应发挥神经保护作用[25]。也有文献[26,27]报道, 这些活性单萜类成分在体内脱去苯甲酰基后可转化为苯甲酸, 并透过血脑屏障发挥抗抑郁作用。由此推测, 苯甲酰基团的脱除可能是单萜类成分在体内发挥抗抑郁作用的关键代谢途径。此外, 本研究发现 BS-60E 中的单萜成分—氧化芍药苷 (L0) 的代谢过程在正常和抑郁大鼠血清中的代谢过程未表现出显著差异, 该结果与课题组前期的研究结论不一致[16]。我们推测, 当药物以混合物 (BS-60E) 形式给药时, 不同成分之间可能存在相互作用, 从而影响了其在体内的吸收与代谢

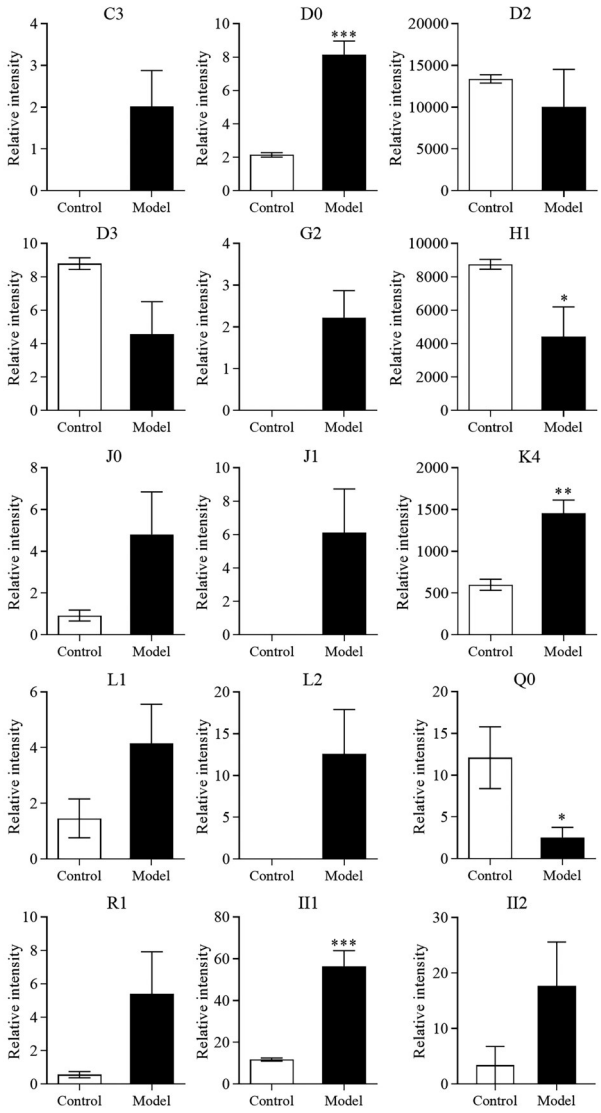


Figure 9 Comparison of the relative contents of differential constituents in urine between normal rats and depressed rats after oral administration of BS-60E. $n = 6$, $\bar{x} \pm s$. $^{*}P < 0.05$, $^{**}P < 0.01$, $^{***}P < 0.001$ *vs* control

过程。

检测到的入血成分中, 多酚类成分主要以原型成分和代谢产物形式存在, 根据其在血清代谢产物的结构特征推测, 该类成分在体内主要经历葡糖基化和葡糖醛酸化等II相代谢反应。研究表明, 儿茶素及其衍生物具有一定的抗抑郁作用[28]。除儿茶素类成分外, 本研究还在大鼠血清中新检出多种没食子酰衍生物类多酚, 且其吸收程度较高。目前尚无该类成分抗抑郁活性的相关报道, 未来可进一步探究其是否具有抗抑郁作用。

本研究初步揭示了BS-60E在正常与抑郁大鼠体内的代谢差异, 为筛选白芍抗抑郁药效物质提供了参考依据。然而, 研究仍存在一定局限性: 本研究仅对BS-60E中的关键原型成分及代谢产物的相对含量进行比较, 未开展绝对含量测定; 大鼠血液与尿液样本采集时间点单一, 未能构建完整的药代动力学曲线; 此外, 主要代谢产物的抗抑郁活性尚未进行验证, 其是否为BS-60E中真实的药效物质仍需进一步确认。因此, 后续研究将围绕上述不足展开, 以更全面阐释白芍抗抑郁的药效物质基础。

作者贡献: 邹忠梅、于猛负责指导、审核与编辑写作、提供资源、获取资助; 何昊奇、郑大华负责调查研究、验证、可视化呈现、初稿写作; 刘帅负责方法论、数据管理。

利益冲突: 所有作者均声明无利益冲突。

References

[1] Chinese Pharmacopoeia Commission. Pharmacopoeia of the People's Republic of China (中华人民共和国药典) [M]. Vol. I. 2025 Ed. Beijing: China Medical Science Press, 2025: 105.

[2] Ma W, Ren H, Meng X, et al. A review of the ethnopharmacology, phytochemistry, pharmacology, pharmacokinetics and quality control of *Paeonia lactiflora* Pall. [J]. J Ethnopharmacol, 2024, 335:118616.

[3] Ren DD, Li WH, Wang X, et al. Research progress on antidepressant effect of tonifying Chinese herbal medicine [J]. Pharm Clin Chin Mater Med (中药与临床), 2023, 14:96-104.

[4] Xue QY, Zhang Y, Li GH, et al. Discussion on medication rules and mechanism of Chinese herbal compound prescriptions for depression based on data mining and network pharmacology [J]. J Guangzhou Univ Tradit Chin Med (广州中医药大学学报), 2024, 41: 2804-2814.

[5] Wang XL, Feng ST, Wang YT, et al. Paeoniflorin: A neuroprotective monoterpenoid glycoside with promising anti-depressive properties [J]. Phytomedicine, 2021, 90: 153669.

[6] Li YC, Zheng XX, Xia SZ, et al. Paeoniflorin ameliorates depressive-like behavior in prenatally stressed offspring by restoring the HPA axis-and glucocorticoid receptor-associated dysfunction [J]. J Affect Disord, 2020, 274: 471-481.

[7] Cong C, Kluwe L, Li S, et al. Paeoniflorin inhibits tributyltin chloride-induced apoptosis in hypothalamic neurons *via* inhibition of MKK4-JNK signaling pathway [J]. J Ethnopharmacol, 2019, 237: 1-8.

[8] Cheng J, Chen M, Wan HQ, et al. Paeoniflorin exerts antidepressant-like effects through enhancing neuronal FGF-2 by microglial inactivation [J]. J Ethnopharmacol, 2021, 274: 114046.

[9] Mu DZ, Xue EM, Xu JJ, et al. Antidepression and prokinetic effects of paeoniflorin on rats in the forced swimming test *via* polypharmacology [J]. Evid Based Complement Alternat Med, 2020, 2020: 2153571.

[10] Zheng DH, Yu M, Jin Z, et al. Identification of the antidepressant

fraction and its major chemical constituents of Radix Paeoniae Alba [J]. Acta Pharm Sin (药学学报), 2023, 58: 1307-1316.

[11] Li GX, He JQ. Study on serum pharmacochemistry of Chinese materia medica and its compound prescriptions [J]. Mod Med Health Res (现代医学与健康研究), 2018, 2: 153.

[12] Tian Y, Chen Q, Lei L, et al. Research progress on the influence of disease on pharmacokinetics of Chinese materia medica [J]. Pharmacol Clin Chin Mater Med (中药药理与临床), 2026, 42: 152-160.

[13] Guo JJ, Qin XM, Liu YT. Research overview of gut bacteria-mediated metabolism of Chinese materia medica [J]. Acta Pharm Sin (药学学报), 2024, 59: 831-839.

[14] Chen YW, Yang ZW, Tian GF, et al. Research progress on transporters and metabolic enzymes-mediated herb-drug interactions [J]. Chin Tradit Herb Drugs (中草药), 2025, 56: 1852-1860.

[15] Wu L, Xing L, Zou Y, et al. UPLC-QTOF-MS based comparison of rotundic acid metabolic profiles in normal and NAFLD rats [J]. Metabolites, 2022, 13: 38.

[16] Jin Z, Zheng DH, He HQ, et al. Comparative study on metabolites of oxypaeoniflorin in normal and depressed rats [J]. Chin Tradit Herb Drugs (中草药), 2024, 55: 2887-2895.

[17] Yu M, Jia HM, Qin LL, et al. Gut microbiota and gut tissue metabolites involved in development and prevention of depression [J]. J Affect Disord, 2022, 297: 8-17.

[18] Du BX, Fu Y, Sun QH, et al. Characterization of efficacy components of Guizhi plus Gegen decoction in intervention of influenza viral pneumonia based on serum pharmacochemistry of Chinese materia medica [J]. Chin J Exp Tradit Med Formulae (中国实验方剂学杂志), 2023, 29: 168-175.

[19] Duan HY. Antidepressant effect and mechanism of oxypaeoniflorin combined with exercise on depressed rats [J]. Mol Plant Breed (分子植物育种), 2023, 21: 6178-6184.

[20] Zhong SZ, Ma SP, Hong ZY. Peoniflorin activates Nrf2/ARE pathway to alleviate the A$\beta_{1\text{-}42}$-induced hippocampal neuron injury in rats [J]. Acta Pharm Sin (药学学报), 2013, 48: 1353-1357.

[21] Nam KN, Yae CG, Hong JW, et al. Paeoniflorin, a monoterpene glycoside, attenuates lipopolysaccharide-induced neuronal injury and brain microglial inflammatory response [J]. Biotechnol Lett, 2013, 35: 1183-1189.

[22] Wang QS, Yan K, Li KD, et al. Targeting hippocampal phospholipid and tryptophan metabolism for antidepressant-like effects of albiflorin [J]. Phytomedicine, 2021, 92: 153735.

[23] Yu L, Wu Y. Mechanism of benzoylpaeoniflorin on cardiac function in rats with myocardial infarction *via* the Nrf2/HO-1 pathway [J]. Lab Anim Sci (实验动物科学), 2022, 39: 44-48.

[24] Wang Y, Yang S, Liu X, et al. Xiongshao Zhitong granules alleviate nitroglycerin-induced migraine by regulating the TRPV1-mediated NLRP3 inflammatory pathway in rats [J]. Phytomedicine, 2025, 142: 156754.

[25] Hou WC. 6'-*O*-Galloylpaeoniflorin Attenuates Inflammatory and Oxidative Stress Induced Injury in Cerebral Ischemia/Reperfusion Model *via* PI3K/Akt/Nrf2 Pathway (没食子酰芍药苷通过PI3K/Akt/Nrf2通路减轻脑缺血再灌注后炎症反应与氧化应激损伤) [D]. Changchun: Jilin University, 2017.

[26] Zhao ZX, Fu J, Ma SR, et al. Gut-brain axis metabolic pathway regulates antidepressant efficacy of albiflorin [J]. Theranostics, 2018, 8: 5945-5959.

[27] Yu JB, Zhao ZX, Peng R, et al. Gut microbiota-based pharmacokinetics and the antidepressant mechanism of paeoniflorin [J]. Front Pharmacol, 2019, 10: 268.

[28] Qin YN, Du JJ, Wu XH, et al. Research progress on the alleviating effects of tea on anxiety and depression [J]. Food Res Dev (食品研究与开发), 2023, 44: 214-219.